Supporting Information

Enhancing Oxygen Evolution Catalysis of Ni_3Se_2 via Trimetallic Modulation

Hao Zhou,[a] Yikai Wang,[a] Hua Wang,[a] Heye Fu,[a] Ranran Li,[a] Yuekai Zhang,[a] Hong Zhao,[a] Cuishuang Jiang,[a] Tingting Yu,[a] Xia Sun,[a] Maoshuai He,[b] Wenxian Wei[c] and Tao Yang*[a]

[a]*School of Environmental and Chemical Engineering, Jiangsu Ocean University, Lianyungang, Jiangsu 222005, P. R. China*

[b]*College of Chemistry and Molecular Engineering, Qingdao University of Science and Technology, Qingdao, Shandong 266042, P. R. China*

[c]*Testing Center, Yangzhou University, Yangzhou, Jiangsu 266042, P. R. China*

Corresponding Author: Tao Yang

Email: yangtao_hit@163.com (T. Yang)

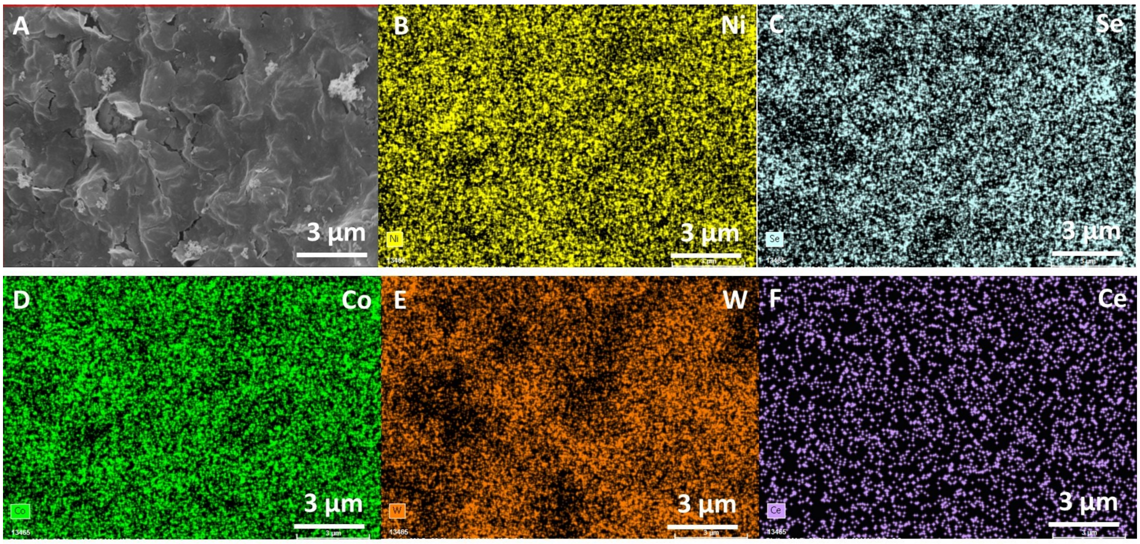

Figure S1. SEM-EDS mapping on (A) CoWCe-Ni_3Se_2, (B) Ni, (C) Se, (D) Co, (E) W and (F) Ce.

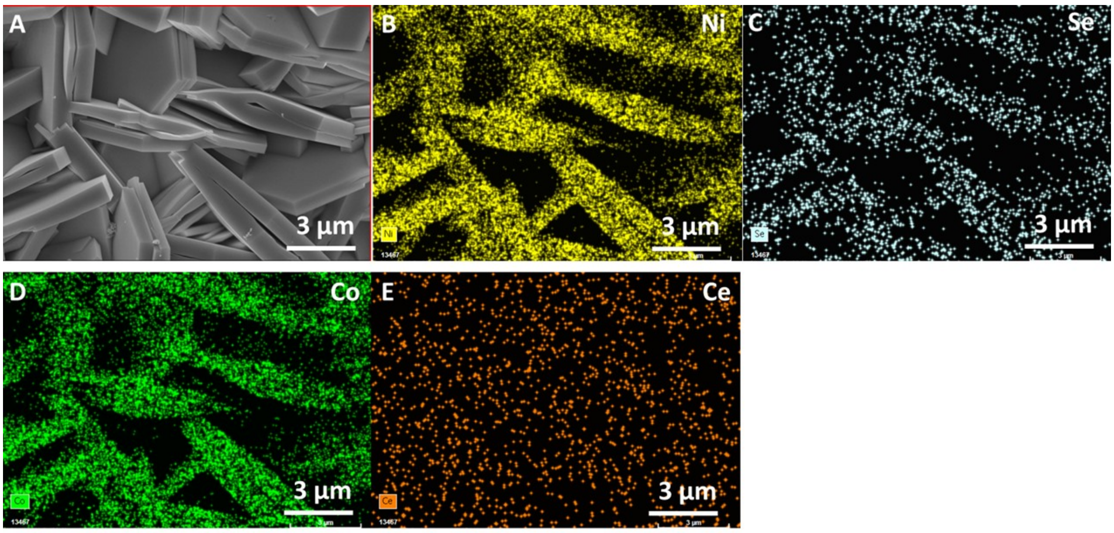

Figure S2. SEM-EDS mapping on (A) CoCe-Ni_3Se_2, (B) Ni, (C) Se, (D) Co and (E)) Ce.

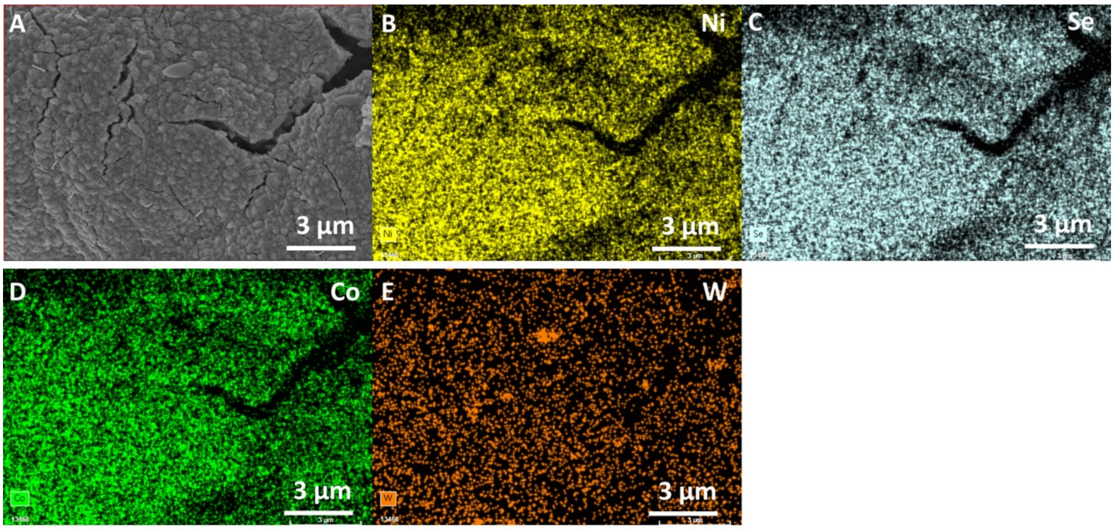

Figure S3. SEM-EDS mapping on (A) CoW-Ni_3Se_2, (B) Ni, (C) Se, (D) Co and (E) W.

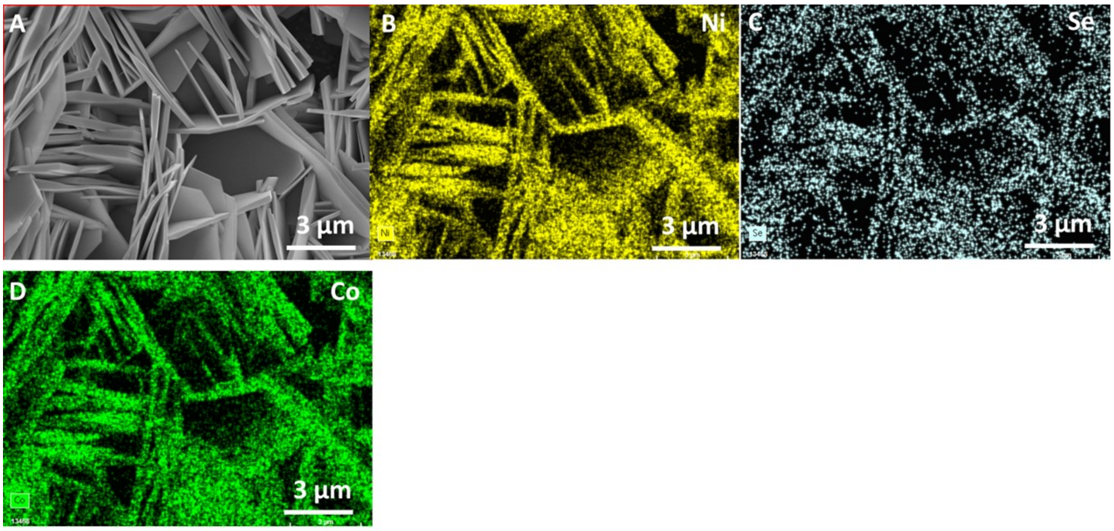

Figure S4. SEM-EDS mapping on (A) Co-Ni_3Se_2, (B) Ni, (C) Se and (D) Co.

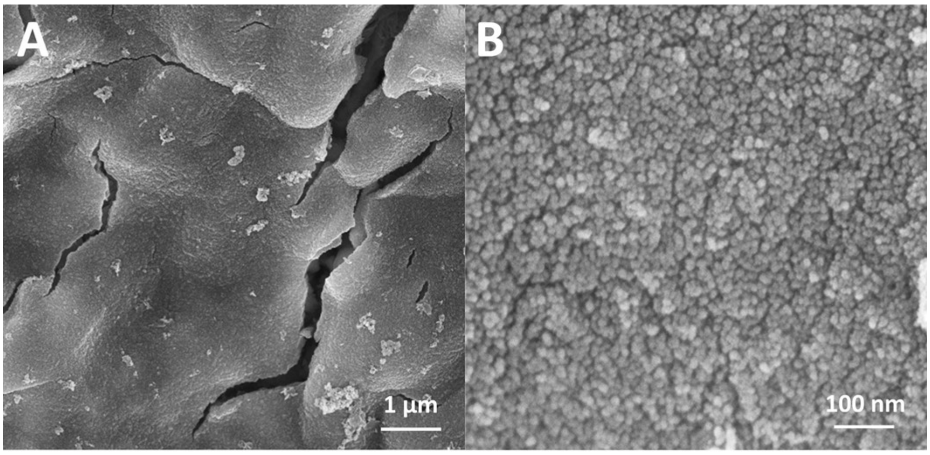

Figure S5. The SEM images of Ni_3Se_2 at (A) low and (B) high magnifications.

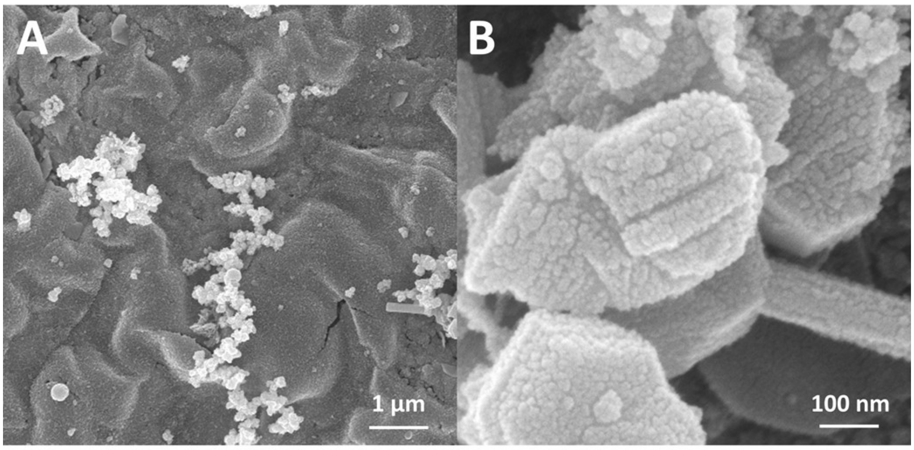

Figure S6. SEM image of WCe-Ni_3Se_2.

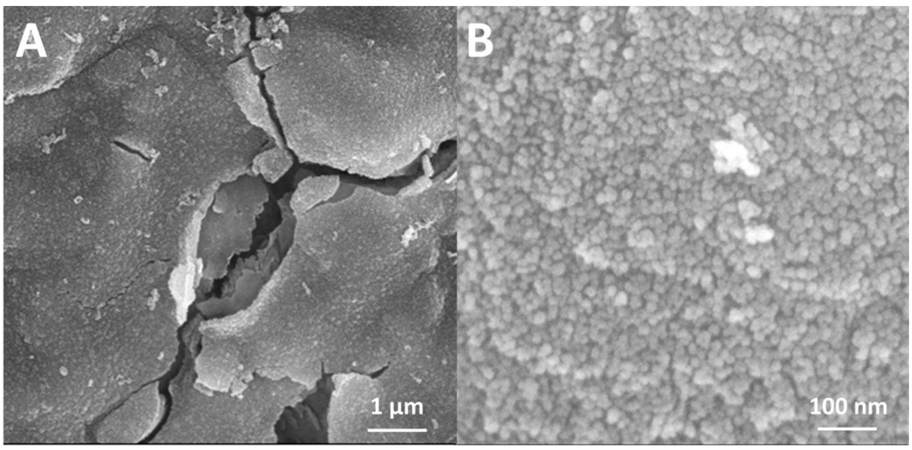

Figure S7. SEM image of W-Ni_3Se_2.

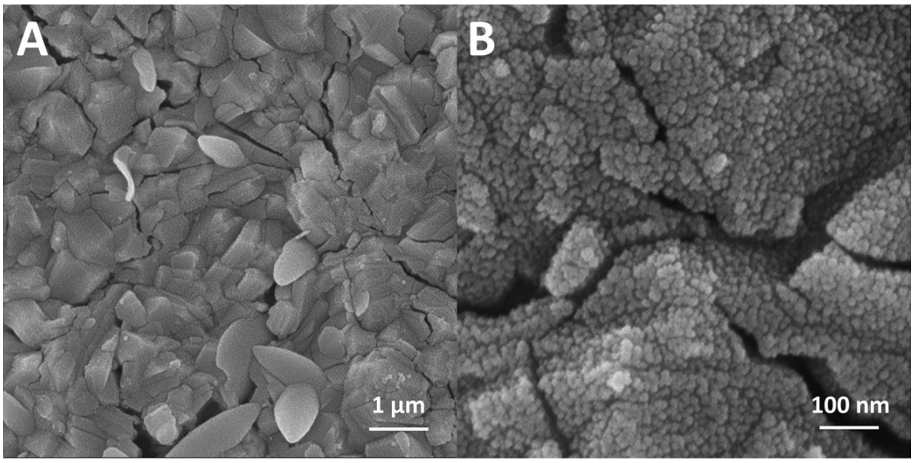

Figure S8. SEM image of W-Ni_3Se_2.

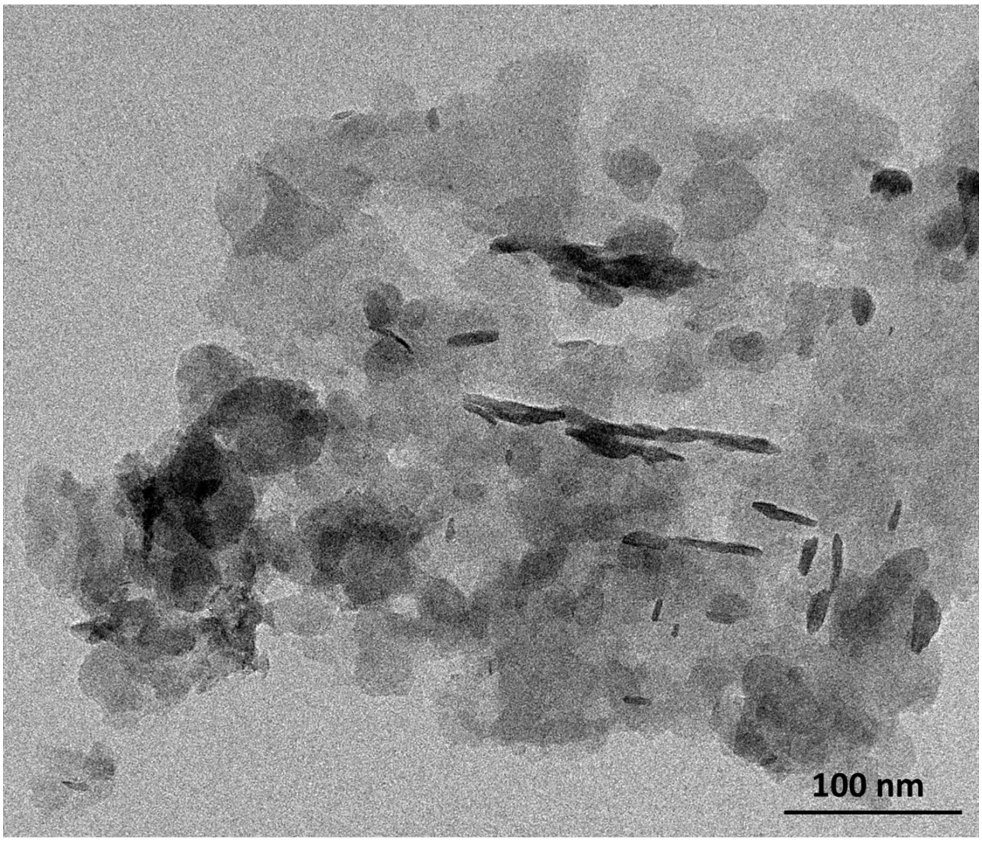

Figure S9 TEM image on CoWCe-Ni_3Se_2.

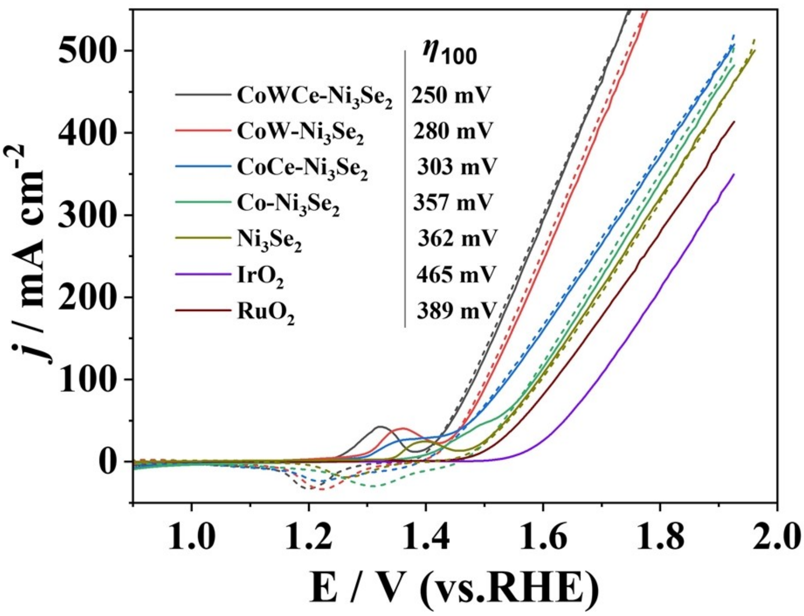

Figure S10. The raw data polarization curves of CoWCe-Ni_3Se_2, CoWCe-Ni_3Se_2, CoCe-Ni_3Se_2, Co-Ni_3Se_2, Ni_3Se_2 and the benchmark catalysts RuO_2 and IrO_2 without iR-compensation. The overpotentials for delivering 100 mA cm^{-2} are listed.

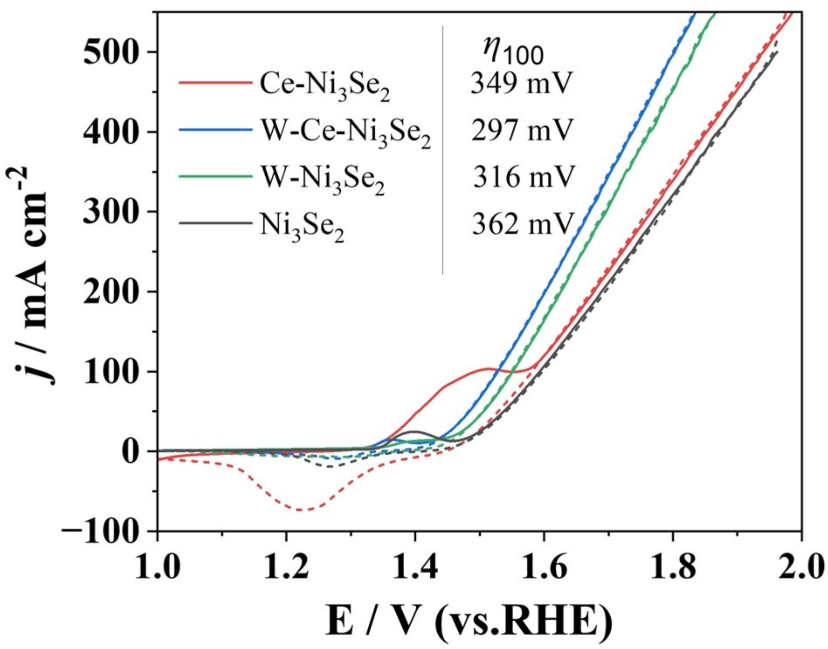

Figure S11. The raw data polarization curves of WCe-Ni_3Se_2, Ce-Ni_3Se_2, W-Ni_3Se_2 and Ni_3Se_2 without iR-compensation.

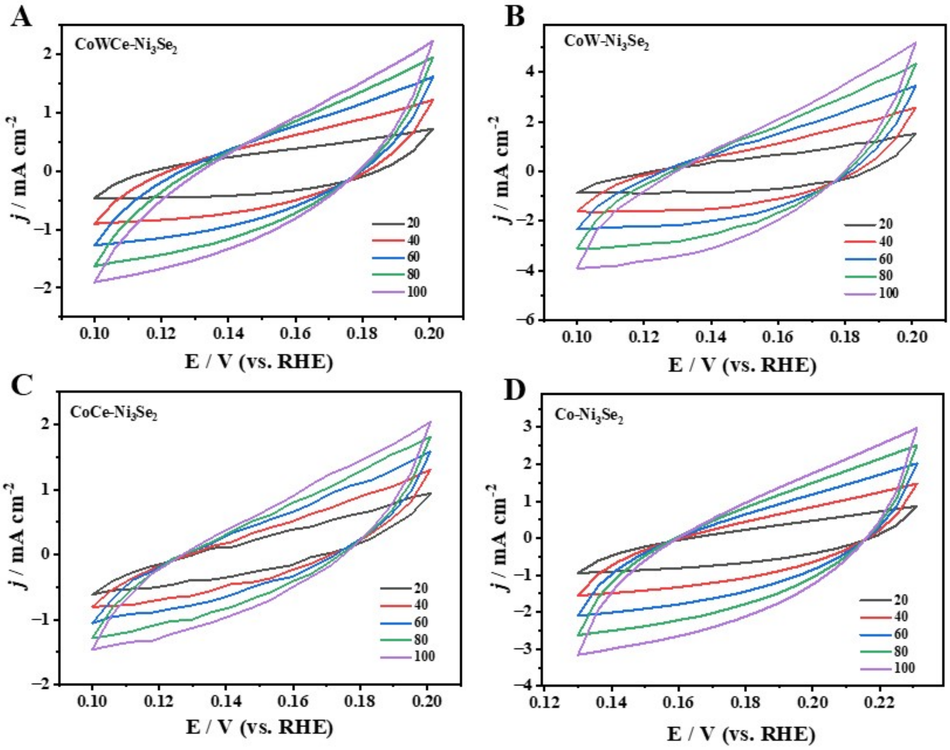

Figure S12. The CV curves of (A) CoWCe-Ni$_3$Se$_2$, (B) CoWCe-Ni$_3$Se$_2$, (C) CoCe-Ni$_3$Se$_2$ and (D) Co-Ni$_3$Se$_2$ for ECSA calculation.

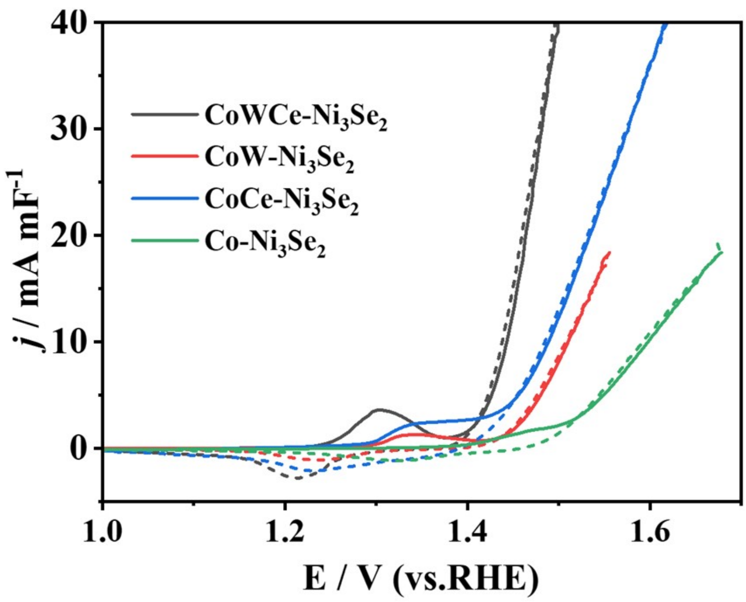

Figure S13. The specific activity curves of CoWCe-Ni$_3$Se$_2$, CoWCe-Ni$_3$Se$_2$, CoCe-Ni$_3$Se$_2$ and Co-Ni$_3$Se$_2$ based on ECSA.

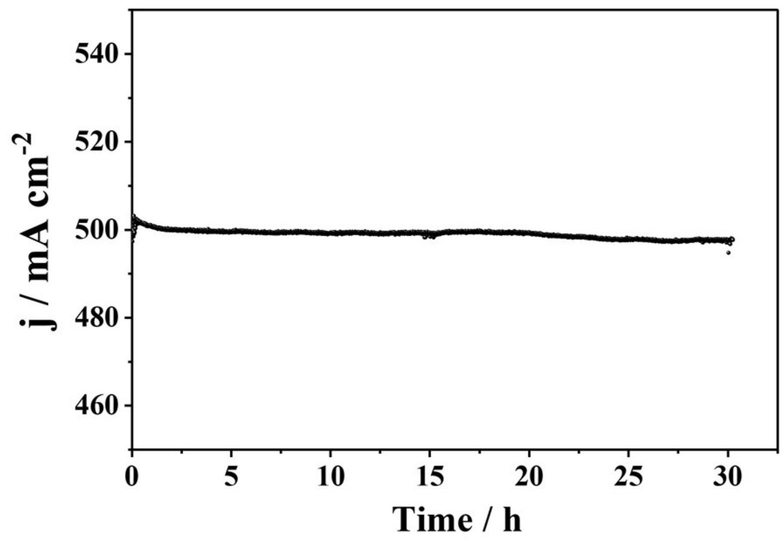

Figure S14. i-t chronoamperometric test of CoWCe-Ni_3Se_2 at 1.729 V for 30 h.

Table S1. The comparison between the present work and the recently reported OER catalysts.

Catalysts	Overpotential at 10 mA cm^{-2} / mV	Tafel slop / mV dec^{-1}	Ref.
CoWCe-Ni_3Se_2	204	33.59	This work
Zn-NiOOH	179	30.8	[1]
FeOOH(Se)	287	54.0	[2]
Fe-Ni3C	275	62.0	[3]
S-NiFe2O4	267	36.7	[4]
N-CoP/CeO2	215	69.0	[5]
Ni0.75Fe0.25Se2	267	67.0	[6]
AlNiCoRuMo	245	54.5	[7]
CoCrFeNiMo	220	59.0	[8]
Mo-NiFeOxHy	193	32.3	[9]

Table S2. The calculated TOF at 1.50 V.

Samples	J@1.50 V mA/cm^2	Sweeping rate V/s	TOF s^{-1}
CoWCe-Ni_3Se_2	499	0.005	0.173858
CoW- Ni_3Se_2	252	0.005	0.080572
CoCe- Ni_3Se_2	140	0.005	0.042919
Co- Ni_3Se_2	39.5	0.005	0.009521

*The number of electrochemically active surface Ni sites was determined by integrating the charge (Q) under the Ni^{2+}/Ni^{3+} redox peak from cyclic voltammetry (CV), assuming a one-electron transfer process per Ni site.

References

[1] Y. Huang, Z. Wang, H. Xiao, Q. Liu, X. Wang, Activating and stabilizing lattice oxygen via self-adaptive zn–niooh sub-nanowires for oxygen evolution reaction, *J. Am. Chem. Soc.* 146 **(2024)** 29006-29016.

[2] S. Niu, W.-J. Jiang, Z. Wei, T. Tang, J. Ma, J.-S. Hu, L.-J. Wan, Se-doping activates feooh for cost-effective and efficient electrochemical water oxidation, *Journal of the American Chemical Society* 141 **(2019)** 7005-7013.

[3] H. Fan, H. Yu, Y. Zhang, Y. Zheng, Y. Luo, Z. Dai, B. Li, Y. Zong, Q. Yan, Fe-doped ni3c nanodots in n-doped carbon nanosheets for efficient hydrogen-evolution and oxygen-evolution electrocatalysis, *Angew. Chem. Int. Ed.* 56 **(2017)** 12566-12570.

[4] J. Liu, D. Zhu, T. Ling, A. Vasileff, S.-Z. Qiao, S-nife2o4 ultra-small nanoparticle built nanosheets for efficient water splitting in alkaline and neutral ph, *Nano Energy* 40 **(2017)** 264-273.

[5] L. Zhang, Y. Lei, W. Xu, D. Wang, Y. Zhao, W. Chen, X. Xiang, X. Pang, B. Zhang, H. Shang, Highly active and durable nitrogen-doped cop/ceo2 nanowire heterostructures for overall water splitting, *Chem. Eng. J.* 460 **(2023)** 141119.

[6] L. Lv, Z. Li, K.-H. Xue, Y. Ruan, X. Ao, H. Wan, X. Miao, B. Zhang, J. Jiang, C. Wang, K. Ostrikov, Tailoring the electrocatalytic activity of bimetallic nickel-iron diselenide hollow nanochains for water oxidation, *Nano Energy* 47 **(2018)** 275-284.

[7] Z. Jin, J. Lyu, Y.-L. Zhao, H. Li, X. Lin, G. Xie, X. Liu, J.-J. Kai, H.-J. Qiu, Rugged high-entropy alloy nanowires with in situ formed surface spinel oxide as highly stable electrocatalyst in zn–air batteries, *ACS Mater. Lett.* 2 **(2020)** 1698-1706.

[8] J. Tang, J.L. Xu, Z.G. Ye, X.B. Li, J.M. Luo, Microwave sintered porous cocrfenimo high entropy alloy as an efficient electrocatalyst for alkaline oxygen evolution reaction, *J. Mater. Sci. Technol.* 79 **(2021)** 171-177.

[9] Y. Wu, Y. Zhao, P. Zhai, C. Wang, J. Gao, L. Sun, J. Hou, Triggering lattice oxygen activation of single-atomic mo sites anchored on ni–fe oxyhydroxides nanoarrays for electrochemical water oxidation, *Adv. Mater.* 34 **(2022)** 2202523.